THERMO PHYSICAL AND FLOW PROPERTIES OF CO_2 HYDRATE SLURRY

O. SARI[1], J. HU[1], S. EICHER[1], P. EGOLF[1], P. HOMSY[2]

[1] Institute of Thermal Engineering (IGT)
University of Applied Sciences of Western Switzerland
Av. des Sports 14, Yverdon-les-Bains, Switzerland,
[2] Nestec, Avenue Nestlé 55, 1800 Vevey, Switzerland
Osmann.sari@heig-vd.ch

ABSTRACT

The apparent viscosity and flow regime of CO_2 hydrate slurry were investigated with a XL7-100 on-line resonant viscometer. Possible reasons for the viscosity changes before and after the nucleation of hydrates are discussed. In addition, super saturation of the CO_2 solution under certain pressure and temperature conditions as well as its density and apparent viscosity were examined. The hydrate's solid fraction and the dissociation enthalpy were evaluated by an on-line Micro DSC system. Real-time coupled multi-electrode array sensor (CMAS) probes were applied to measure the maximal localized corrosion rate of three different materials subjected to CO_2 hydrate slurry and saturated CO_2 solution in the temperature range of 1 to 18 °C and pressure range of 25 to 30 bar. The density of CO_2 hydrate slurry was also experimentally investigated and the relation between the density and the solid fraction has been established.

1. INTRODUCTION

The synthetic refrigerants impact on the environment and newly imposed safety measures force the cooling industry to seek for solutions to remove certain gases or to decrease their content in numerous different systems. During the last ten years the load reduction of refrigerants in installations and the development and use of natural, non-flammable and environment preserving cooling agents became the two preferred methods to improve the current situation. The creation of hydrates – a kind of multifunctional thermal fluid – is one of these promising technologies.

CO_2 hydrates are obtained by the combination of water and CO_2 (gas) under defined conditions of temperature and pressure. CO_2 hydrate slurry is one of the promising recently proposed secondary refrigerants in order to phase out CFC's and HCFC's. CO_2 hydrate slurry is suitable for cooling applications, because its melting point is adjustable by changing the production conditions and can be even applied to the positive temperature range (+5 to +7 °C), which are temperatures required in air-conditioning systems. Pure CO_2 hydrate has a dissociation enthalpy of 500 kJ/kg of water, being 1.5 times higher than that related to the ice crystal melting. In order to use CO_2 hydrate slurry efficiently, not only the intrinsic thermal properties must be known but also rheological data is required.

CO_2 hydrate slurry is produced by high pressure CO_2 gas injection in a cooled water solution. Note that here CO_2 is recovered from existing industrial processes, for example fermentation, and is not specially produced for the purpose. The process could contribute to replace polluting fluids that will be prohibited from the beginning of the year 2010 on in the EU countries. Consequently, a high potential market is arising.

The objective of this paper is to present recent results and new findings regarding density, apparent viscosity, dissociation enthalpy, corrosion rate of CO_2 hydrate slurry in order to prove that CO_2 hydrate slurry as an environmental friendly refrigerant has thermal physical characteristics that are well-suited for refrigeration applications, especially in the field of air conditioning.

2. CO_2 HYDRATE AND CO_2 HYDRATE SLURRY PROPERTIES

2.1 CO_2 Hydrate

Hydrates are non-stoichiometric crystalline compounds formed by cavities of "host" water molecules. Under certain pressure and temperature conditions they are strongly hydrogen bonded with a small guest molecule hydrate structure. There are two types of CO_2 hydrate, namely hydrate I with structure I and hydrate II with structure II respectively. Hydrate I is the most common structure occurring in CO_2 hydrates. Hereafter, only hydrate I will be referred to as CO_2 hydrate. The chemical reaction equation for the hydration is:

$$CO_2 + n\ H_2O \rightarrow CO_2 nH_2O, \tag{1}$$

where n is the hydration number: $5 < n < 7$.

2.2 Density of CO_2 Solution

The density model proposed by Duan *et al.* (2008) for liquid CO_2-H_2O mixtures, hereafter referred as CO_2 solution, was defined using the equation:

$$\rho_{CO2HO} = \frac{M_{CO_2-H_2O}}{V_{CO_2-H_2O}} \tag{2}$$

$$M_{CO_2-H_2O} = x_{CO_2} M_{CO_2} + x_{H_2O} M_{H_2O_2} \tag{3}$$

$$V_{CO_2-H_2O} = V_1\left[1 + (A_1 + A_2 P) x_{CO_2}\right] \tag{4}$$

$$A_i = A_{i1}T^2 + A_{i2}T + A_{i3} + A_{i4}T^{-1} + A_{i5}T^{-2} \qquad (i=1,2) \tag{5}$$

$\rho_{CO2\text{-}H2O}$ is the density of the CO_2 solution, $V_{CO2\text{-}H2O}$ is the molar volume of the CO_2 solution, P is the pressure (in MPa), T the temperature (in K) and M and x are the molar mass and the mole fraction, respectively. The mole fractions are calculated as:

$$x_{CO2\text{-}} = \frac{\frac{m_{CO_2}}{M_{CO_2}}}{\frac{m_{CO_2}}{M_{CO_2}} + \frac{1}{M_{H_2O}}} \tag{6}$$

and

$$x_{H2O\text{-}} = 1 - x_{CO2\text{-}} \tag{7}$$

where m_{CO_2} is the CO_2 solubility in water (in g/g) proposed by Duan *et al.* (2006).

2.3 Density of CO_2 Hydrate Slurry

The density of hydrate slurry can be derived from a mass balance where the mass of free CO_2 gas in the hydrate slurry can be neglected due to the very small amount and not considered in the equation:

$$\rho_{hydrate,slurry} = \frac{\rho_{liquid} \cdot \rho_{hydrate}}{\rho_{liquid} \cdot x_{hydrate} + \rho_{hydrate}\left(1 - x_{hydrate}\right)} \text{ and } x_{liquid} + x_{hydrate} = 1 \tag{8}$$

where ρ is the density, m is the mass, x_{liquid} is the liquid mass fraction in the hydrate slurry and $x_{hydrate}$ is the hydrate concentration (solid fraction) in the hydrate slurry.

2.4 Viscosity of CO_2 Solution

The viscosity of the CO_2 solution was reproduced using the simple empirical equation proposed by Grunberg and Nissan (1949):

$$\eta_{CO2\text{-}H2O} = exp(x_{CO2} \ln \eta_{CO2} + x_{H2O} \ln \eta_{H2O} + x_{CO2}(1 - x_{CO2}) * G) \tag{9}$$

η_{H2O} and η_{CO2} are viscosity of water and CO_2 respectively. G is the only adjustable parameter that can be calculated from experimental results.

2.5 Viscosity of CO_2 Hydrate Slurry

Up to now, not so much information is available regarding the viscosity of CO_2 hydrate slurry. Only few authors have experimentally investigated the viscosity of CO_2 hydrate slurry. Oyama *et al.* (2003) argue that the large number of water molecules tends to construct precursor hydrogen-bonded structures in the solution leading to an increase in the viscosity prior to the hydrate formation. Andersson (1999) and Andersson and Dudmundsson (2000) have also reported that the slurry viscosity increases with increasing hydrate concentration.

2.6 Enthalpy of Hydrate Fusion

The formation of gas hydrate is an exothermic equilibrium process. The dissociation of gas hydrate is an endo-thermic equilibrium process. To use this endothermic process is to benefit from the latent heat of fusion of the CO_2 hydrate phase change. As an example, Bozzo *et al.* (1975) have reported an enthalpy of dissociation of 58.16 kJ/mol at 10 ºC and for the carbon dioxide hydrates a hydration number of 7.03.

3. EXPERIMENTAL LOOP AND MEASUREMENT FACILITIES

An experimental loop was built up to study production, storage, transport and use of CO_2 hydrate slurry as newly developed refrigerant. In addition the loop is used to characterise the thermal-physical properties of the CO_2 hydrate slurry.

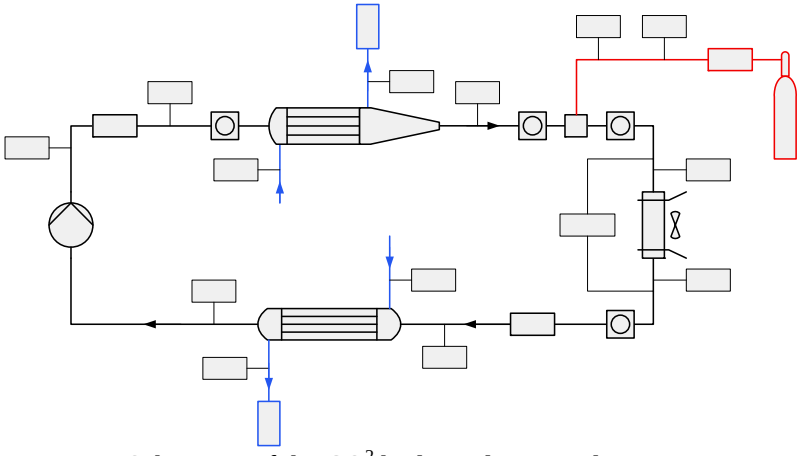

Figure 1 Schematic of the CO^2 hydrate slurry production system

As shown in Figure 1, CO_2 hydrate slurry loop (in black): It is equipped with a high-pressure pump (2), two high pressure, shell-and-tube heat exchangers (4 and 5), heater (6) and CO_2 gas injection unit (3). Among these two heat exchangers, (4 will be used for hydrate production and (5) will be used as a cooler to cool down the temperature of solution. Four visualisation windows, X1, X2, X3 and X4; CO_2 gas circuit (in red): a CO_2 bottle feeds the gas circuit to the one single injection point of the CO_2 hydrate slurry loop. Gas temperature is monitored by one K-type thermocouple (T_{11}), pressure will be recorded by transducer (P_2) and mass flow rate is recorded by mass flow meter (M_1). Neutragel/water cooling loops (in blue) for shell side of two heat exchangers. There are two chillers (not displayed in Figure 1) using neutragel/water 30% as coolant to cool down (or heat up) the two heat exchangers (4) and (5);

Temperature in the loop was monitored by new temperature sensor developed in collaboration with Roth + CO AG. The objective was to obtain a high precision temperature measurement in a point. The mass flow rate of all working fluids in the experimental rig was measured by Endress+Hauser mass flow meters. They are M1, M3, M4, M5, and M6 respectively. Densities of water, CO_2 solution as well as CO_2 hydrate slurry are measured by mass flow meters of Endress+Hauser, which were calibrated according to the suitable temperature and pressure range for hydrate formation and dissociation. The heat capacity and enthalpy of hydrate slurry are measured by a digital scanning calorimetry (DSC). There is a new innovative device XL7-100 viscometer to measure on-line the fluid viscosity. The XL7-100 viscometer produced by Hydramotion Ltd. in UK is a class of instruments called vibrational or resonant viscometers. Real-time coupled multi electrode array sensor (CMAS) probes were

M5
T1
X1
M3
4
P1
T3
Axima Heat Exchanger
Pumpe 2

used to measure the maximal localised corrosion rate of type 1018 low carbon steel, copper 110 and 304L stainless steel in CO_2 hydrate slurry and saturated CO_2 solution in the temperature range 1 to 18 °C and pressure range 25 to 30 bar.

4. RESULTS AND DISCUSSION

4.1 Density and Viscosity Results

Density and viscosity of water

The density and viscosity of tap water under atmosphere and dynamic conditions was measured online by a mass flow meter at temperatures between 1 and 29 °C. The temperature of the water in the loop was first set at 29 °C and then cooled down continuously to 1 °C. The velocity of water in the loop was about 1 m/s driven by a high pressure pump. This experiment was repeated three times under the same experimental conditions to evaluate the measurement deviations. The maximal deviation between the density measurements was estimated to be 2.2 %. As expected, the density decreases with increasing temperature. Results obtained from water EoS proposed by Wagner and Pruess (2002) were used for comparison purposes. The experimental values are in a good agreement with the literature data with a maximal deviation of 5.5 % found at lower temperatures. Measurement of the viscosity of tap water under atmospheric conditions was performed to evaluate the "resonance" method of the XL7-100 viscometer, employed to record online the fluid viscosity. The maximal deviation between measurements was estimated to be 3.5 %. The experimental values are in good agreement with the viscosity equation proposed by Watson *et al.* (1980) and the absolute deviation is within 4 %. The "resonance" method, which is proposed in this study, can be applied to determine the viscosity of the fluid with a maximal uncertainty of 4.5 %.

Density and viscosity of the CO_2 solution

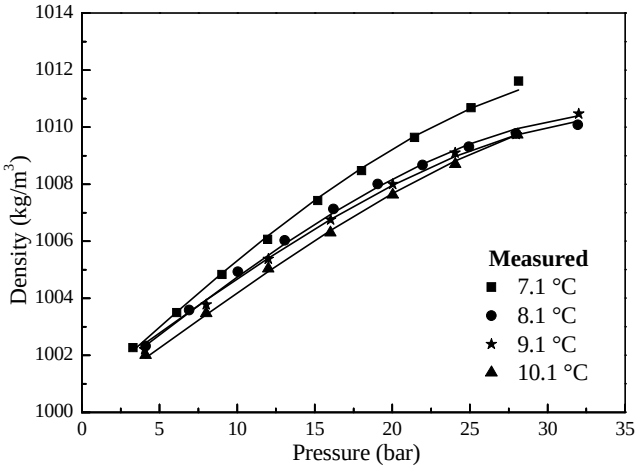

Figure 2a Density of the CO_2 solution as function of pressure and temperature.

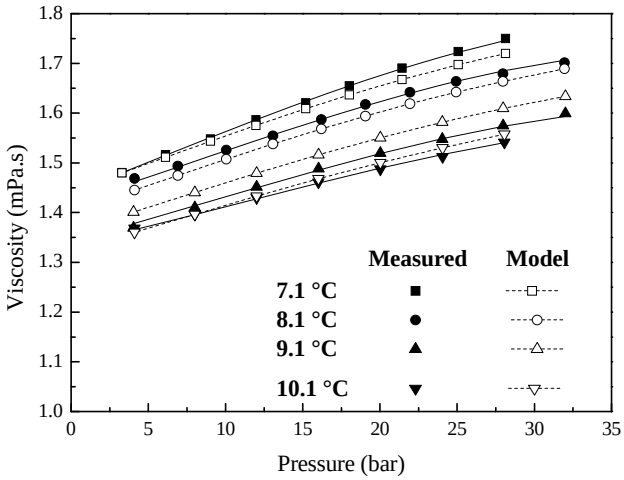

Figure 2b The pressure and temperature dependence of the CO_2 solution viscosity.

CO_2 solution density and viscosity measurements were also undertaken at four different temperatures: 7, 8, 9 and 10 °C. Figure 2a shows the temperature and pressure dependence of the density of the CO_2 solution. It can be seen that density decreases with increasing temperature, but increases with increasing pressure. It follows the behaviour reported by other investigators such as Garcia (2000), who also indicated that CO_2 saturated water was heavier than ordinary water. In a similar manner to the density description, from Figure 2b we can see that the viscosity of the CO_2 solution was also found to decrease with increasing temperature and to increase with increasing pressure. This indicates that high pressures and low temperatures aid more CO_2 gas to be dissolved into water, resulting in a higher viscosity of the solution. In other words, the viscosity of the CO_2 solution depends on the CO_2 solubility.

Experimental results were also compared with Grunberg and Nissan's (1949) correlation for viscosity of liquid mixtures. The only adjustable parameter in this equation, *G*, was calculated using the experimental data and

literature values for viscosity of CO_2 gas and water. The parameter G was found to be dependent on the CO_2 mole fraction and was therefore described using a polynomial function.

Viscosity of CO_2 solution and CO_2 hydrate slurry at different density values

The tap water in the experimental loop was cooled down simultaneously by two chillers to 1.5 °C. The velocity of the water was about 1 m/s. Afterwards, CO_2 gas was injected into the water several times to form a CO_2 solution and, thereafter, a CO_2 hydrate slurry (see in Figure 3, which shows the general appearance of the CO_2 hydrate slurry). The temperature setting for the two chillers was kept at 1 °C during the whole experiment. The safety pressure regulation for the loop is 37 bar. After each injection, fluid in the loop was left to stabilize for several minutes. The temperature, pressure, viscosity and density of water, saturated CO_2 solution as well as CO_2 hydrate slurry were measured, the average values of the above variables under stable conditions were derived, see Figure 4, where each scan corresponds to 5 seconds.

Figure 3 Appearance of CO_2 hydrate slurry.

From Figure 4a and 4b, it can be seen that during the entire experiment, the fluid underwent three different states, namely liquid water, CO_2 solution, and CO_2 hydrate slurry, respectively. However, the temperature of the fluid was not much influenced by the phase transition and was regulated by the two chillers whose fluctuations varied between 1.5 to 2.3 °C.

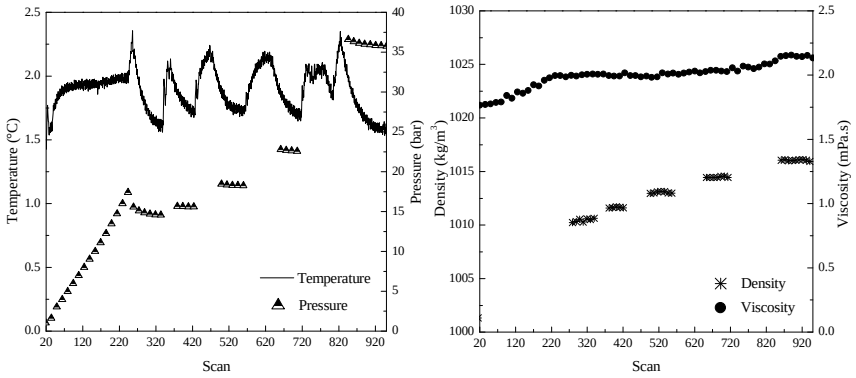

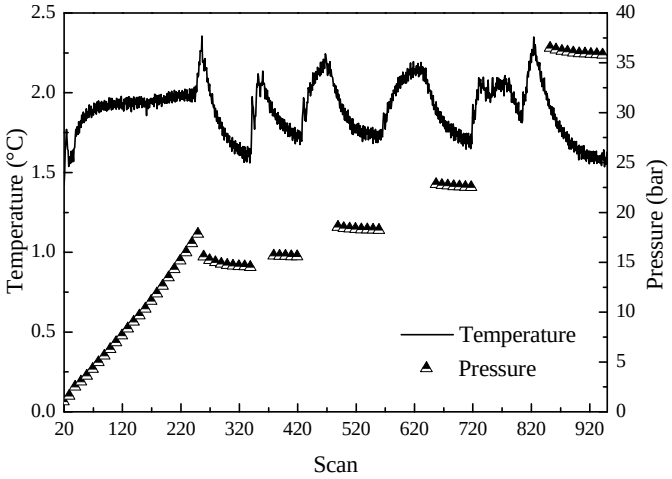

Figure 4a Temperature and pressure profile in the loop during the experiment

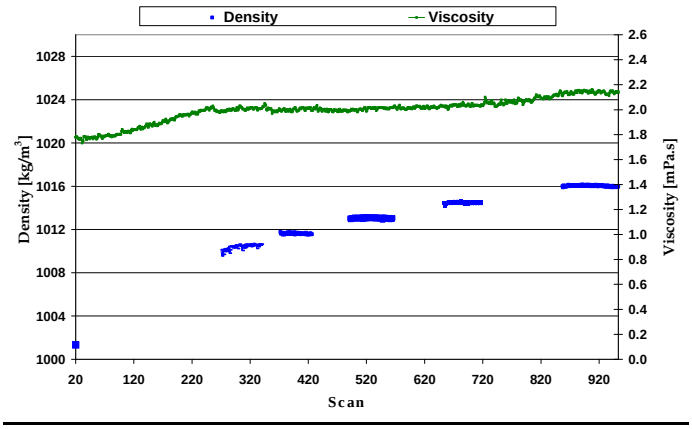

Figure 4b Viscosity as function of solution density during the experiment

Initially the water in the loop was at 1 bar and 1.5 °C for which a viscosity of 1.78 mPa.s and a density of 1001.2 kg/m^3 were recorded. During several injections of CO_2 gas into the closed circuit, the pressure in the loop was gradually increased. This was followed by an increase in the viscosity and density of the fluid. Hydrate formation was only detected after scan 258 when the CO_2 solution changed into CO_2 hydrate slurry. A pressure drop of about 2.5 bar was observed during the formation of hydrates. The properties of water, CO_2 solution and CO_2 hydrate slurry are compared at different loop conditions in Table 1.

Table 1 Properties for water, CO_2 solution and CO_2 hydrate slurry at different loop conditions.

Fluid	**Average Pressure (bar)**	**Temperature range (°C)**	**Average Density (kg/m^3)**	**Average Viscosity (mPa.s)**
Water	1	1.5	1001.2	1.78
CO_2 solution	1-17.6 (unstable)	1.5-2	1001.2-1010 (unstable)	1.78-2
CO_2 hydrate slurry	14.7	1.6 - 2.2	1010	2
CO_2 hydrate slurry	15.6	1.7-2.0	1011.6	2
CO_2 hydrate slurry	18.3	1.7-2.0	1013	2.01
CO_2 hydrate slurry	22.6	1.75-2.0	1014.5	2.01-2.05
CO_2 hydrate slurry	36	1.6-1.95	1016	2.14

This experiment shows that within the temperature range of 1.5 to 2 °C, as pressure increases, so does the average density and viscosity of the fluid. However, after formation of CO_2 hydrates in the solution, despite the large increase of pressure in the loop (14.7 to 36 bar), the density of the fluid varied from 1010 to 1016 kg/m^3, while the viscosity of the fluid only increased 7 %. This implies that CO_2 hydrate solid particles may contribute only slightly to the viscosity increase. In contrast, when the initial water transformed into the CO_2 solution prior to CO_2 hydrate formation within the same temperature range of 1.5 to 2 °C, pressure was increased from 1 to 17.6 bar, the density from 1001.2 to 1010 kg/m^3, while the increase of viscosity was about 12 %. This suggests that the number of dissolved CO_2 molecules increases with the increase of pressure as well as the interaction between the CO_2 molecules and the water molecules, which will result in a viscosity increase. In addition, in this temperature range, when the CO_2 gas pressure is high (over 15 bar) a large number of hydrogen-bonded CO_2 hydrate precursor may form in the solution before nucleation of hydrates that also cause the increase of viscosity. These results provide evidence to the arguments advanced by Uchida *et al.* (2003) and Oyama *et al.* (2003).

4.2 Dissociation Enthalpy of CO_2 Hydrate

Preliminary measurements of specific heat of tap water were performed with the Micro DSC VII to test the accuracy and reliability of the procedure before applying it to measure dissociation enthalpy of CO_2 hydrate. Within narrow limits, the same pattern is obtained in both curves. Reported values of specific heat of water varied from 4.178 to 4.211 J/kg.K in the chosen temperature range, while the DSC measurements varied from 4.196 to 4.240 J/kg.K with a standard deviation of 0.00929 J/kg.K, which agrees within 0.7 % from reported values in the same temperature range.

Measurements of CO_2 hydrate-ice mixture

Pure CO_2 hydrates are not easy to be generated inside a DSC due to constraints related to the required high pressure conditions and appropriate scanning characteristics. To reduce these complexities, CO_2 hydrate-ice mixture formation and dissociation was performed to obtain the dissociation enthalpy of pure CO_2 hydrate. Based on the described preliminary measurements, a DSC experimental procedure for the CO_2 hydrate-ice mixture was applied. Tap water mass was accurately weighed; a simple pressure panel was adapted to guarantee CO_2 gas pressure around 15 bar during the formation and dissociation process; the Micro DSCVII was cooled down to -15 °C with a scanning rate of 0.08 K/min to allow water crystallization and CO_2 hydrate formation; then the Micro DSCVII was heated up to 25 °C at a slow scanning rate of 0.15 K/min. After the ice melting, an endothermic peak linked with CO_2 hydrate dissociation was detected.

Figure 5a shows two exothermic peaks. The first large one corresponds to ice formation, while the second one relates to CO_2 hydrate formation. Ice formation occurs prior to hydrate formation. Since ice is easier to form in the DSC, a large portion of water formed ice, released a large amount of heat and only a small portion of water formed CO_2 hydrate. This explains the difference of sizes between the two observed peaks. Figure 5b shows two endothermic peaks. The first large one corresponds to ice dissociation process and the second one relates to CO_2 hydrate dissociation. Ice dissociation occurs prior to hydrate formation. Figure 5b also reveals that the mixture is mainly composed of ice since the area (which equals energy) of the first peak is much larger than the one of the second peak. By integrating the area of the second peak, a CO_2 hydrate dissociation enthalpy value of 493 kJ/kg water is achieved, which is in very good agreement with the value measured by Marinhas *et al.* (2007), who reported a hydrate enthalpy equal to 500 kJ/kg of water.

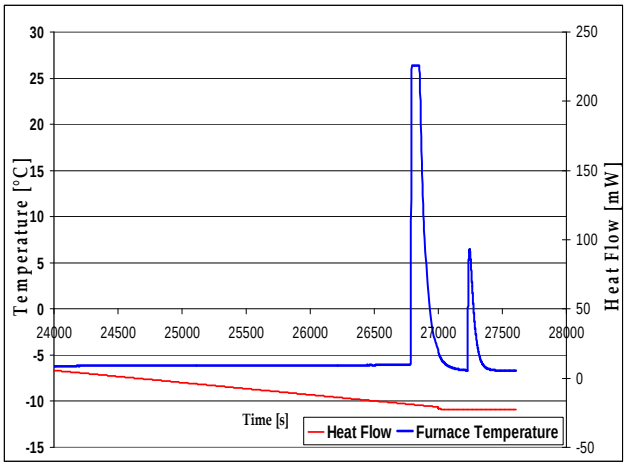

Figure 5a The Formation of Ice and CO_2 Hydrate Mixture Micro DSCVII under 15 bar. The first peak refers to ice formation and the second peak refers to hydrate formation

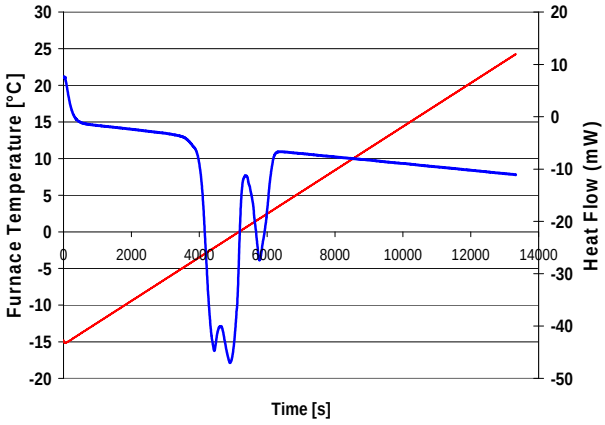

Figure 5b The Dissociation of Ice and CO_2 Hydrate Mixture in the Vessel of the Micro DSCVII; the first peak refers to ice melting while the second peak refers to CO_2 hydrate dissociation

4.3 Corrosion Rate of CO_2 Hydrate Slurry

During the experiment, several pH tests were carried out and values of saturated CO_2 solution as well as CO_2 hydrate slurry was found to be between 5.5 and 6. That means that the CO_2 solution and CO_2 hydrate slurry are both weak acidic substances. To study the corrosion effects of the CO_2 solution as well as the CO_2 hydrate slurry

on low carbon steel, stainless steel and copper for the (future) air-conditioning industry, a complete cycle (creation and dissociation) of CO_2 hydrate slurry was conducted, which included: cooling down the saturated CO_2 solution from room temperature to a temperature around 1 to 2 °C and at a pressure range of 25 to 30 bar; injection of CO_2 gas to reach super saturation conditions; formation and cycling CO_2 hydrate slurry in the loop until the hydrate slurry reaches a temperature of approximately 6 °C; consuming of CO_2 hydrate slurry in the heat exchanger at a temperature above 6 °C until all CO_2 slurry dissociates (around 9 °C).

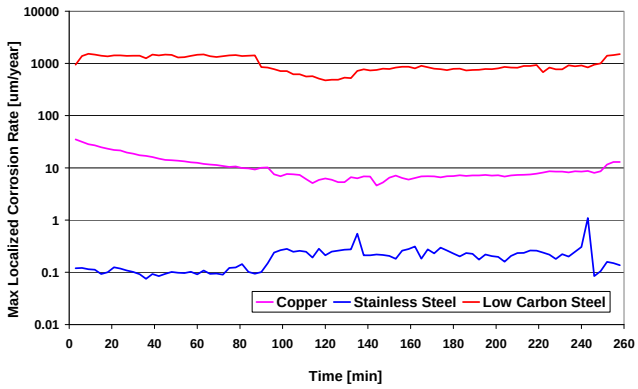

Figure 6a Maximum Localised Corrosion Rates of Different Material Probes during a Short-Term Testing in the CO_2 Hydrate Slurry Loop

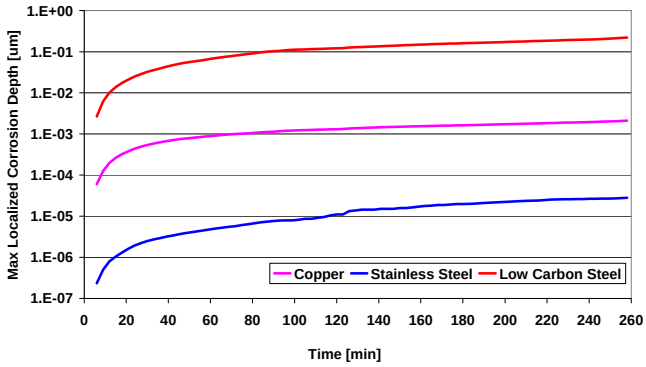

Figure 6b Maximum Localised Corrosion Penetration Depth Measured from the Probes

With the aid of probe tube fittings, the high pressure CS1018 low carbon steel, copper 110 and 304L stainless steel probes were vertically immersed in the CO_2 hydrate slurry transportation pipes. The experiments were conducted at a temperature ranging from 1 to 18 °C and pressure ranging from 25 to 30 bar. High pressure probes were subjected to a complete cycle of CO_2 hydrates slurry formation and dissociation and transferred signals to CMAS analyzer S-50. For stabilisation purposes, CMAS was turned on for more than two hours before monitoring.

Figure 6a shows the maximal localised penetration rates for type 304L stainless steels, type copper 110 and type 1018 low carbon steel . The stabilised maximum localised corrosion rates for the three metals varied by nearly 5 orders of magnitude. Short-term experimental results show that type 304L stainless steel and copper 110 displayed very good resistance to the corrosion caused by CO_2 hydrate slurry, while type 1018 low carbon steel had very poor resistance to the corrosion. The maximum localised corrosion penetration depths are shown in Figure 6b. Metal damage on the 304L stainless steel was smallest while on the 1018 low carbon steel it was largest.

5. CONCLUSIONS AND OUTLOOK

By testing with water, all measurement devices and techniques employed in this work were shown to be reliable and repeatable. The density and viscosity of the CO_2 solution were found to decrease with increasing temperature and increase with increasing pressure. High pressures and low temperatures conditions were found to favour the dissolution of CO_2 gas into water resulting in higher viscosity of the solution. In other words, the viscosity of the CO_2 solution depends on the CO_2 solubility. Formation of the CO_2 hydrate slurry from saturated CO_2 solution revealed that the CO_2 hydrate solid contributes only slightly to the viscosity increase resulting in excellent pumpability characteristics regarding power consumption even for a very high density. Experimental results also imply that the interactions between CO_2 molecules and water molecules are dependent on the pressure and temperature conditions and, therefore, influence the viscosity. A large number of hydrogen-bonded CO_2 hydrate precursor, which may form in the supersaturated solution before nucleation of hydrates also cause the increase of viscosity. The density of CO_2 hydrate slurry depends on the solid concentration of pure hydrates. At a suitable hydrate formation temperature range, the density of CO_2 hydrate slurry increases with increasing

pressure. The CO_2 hydrates dissociation enthalpy was measured by means of a DSC and equals 493 kJ/kg of water, which is in good agreement with the available literature data. On-line measurement of corrosion rate have demonstrated that although CO_2 hydrate slurry is a kind of weak acidified substance, it still has negative effects on three test metals when considering a long term application. Experimental results in this paper provide important reference data in selecting different materials for the applications of CO_2 hydrate slurry in air conditioning industry, cold storage and other applications. In the near future, on-line measurement of thermal conductivity will be carried out; and an equation of viscosity of CO_2 hydrate slurry as a function of the solubility will be established.

ACKNOWLEDGEMENTS

We acknowledge the financial support of the Office Fédéral de l'Energie (OFEN) Switzerland, Commission pour la promotion de la Technologie et l'Innovation (CTI), Switzerland and the "*Haute Ecole de Suisse Occidentale*" (HES-SO).

REFERENCES

1. Duan, Z., Hu, J., Li, D. and Mao, S., 2008, *Density of the CO_2-H_2O and CO_2-H_2O-NaCl Systems Up to 647 K and 100 MPa*, Energy and Fuels.
2. Duan, Z., Sun, R., Zhu, C. and Chou, I-M., 2006, *An Improved Model for the Calculation of CO_2 solubility in Aqueous Solutions Containing Na^+, K^+, Ca^{2+}, Mg^{2+}, Cl^- and SO^{2-4}*, Marine Chemistry, **98**, p. 131-139.
3. Grunberg, L. and Nissan, A.H., 1949, *Mixture Law for Viscosity*, Nature, **164**(4175), p. 799-800.
4. Oyama, H., Ebinuma, T., Shimada, W., Takeya, S., Nagao, J., Uchida, T. and Narita, H., 2003, *An Experimental Study of Gas-Hydrate Formation by Measuring Viscosity and Infrared Spectra*, Can. J. Phys. , **81**, p. 485-492.
5. Andersson, V., 1999, *Flow Properties of Natural Gas Hydrate Slurries. An Experimental Study.*, Petroleum Engineering and Applied Geophysics, Norwegian University of Science and Technology, PhD Thesis.
6. Andersson, V. and Gudmundsson, J.S., (2000). Flow *Properties of Hydrate-in-Water Slurries*, Ann.N. Y. Acad. Sci., **912**, p. 322-329.
7. Bozzo, A.T., Chen, H.-S., Kass, J.R. and Barduhn, A.J., (1975), *The properties of. the hydrates of chlorine and carbon dioxide*, Desalination ,16, p. 303–320.
8. Wagner, W. and Pruss, A., 2002, *The IAPWS Formulation 1995 for the Thermodynamic Properties of Ordinary Water Substance for General and Scientific Use*, J. Phys. Chem. Ref. Data, **31**(2), p. 387-535.
9. Watson, J.T.R., Basu, R.S. and Sengers, J.V., 1980, *An Improved Representative Equation for the Dynamic Viscosity of Water Substance*, J. Phys. Chem. Ref. Data, **9**(4), p. 1255-1290.
10. Garcia, J.E., 2001, *Density of Aqueous Solutions of CO_2*, Lawrence Berkeley National Laboratory, University of California, California.
11. Uchida, T., Ohmura, R., Nagao, J., Takeya, S., Ebinuma, T. and Narita, H., 2003, *Viscosity of Aqueous CO_2 Solutions Measured by Dynamic Light Scattering*, J. Chem. Eng. Data, **48**, p. 1225-1229.
12. Marinhas, S., Delahaye, A., Fournaison, L., Dalmazzone, D., Furst, W. and Petitet, J-P, 2006, *Modelling of the Available Latent Heat of a CO_2 Hydrate Slurry in an Experimental loop Applied to Secondary Refrigeration*, Chem. Eng. and Processing, **45**, p. 184-192.